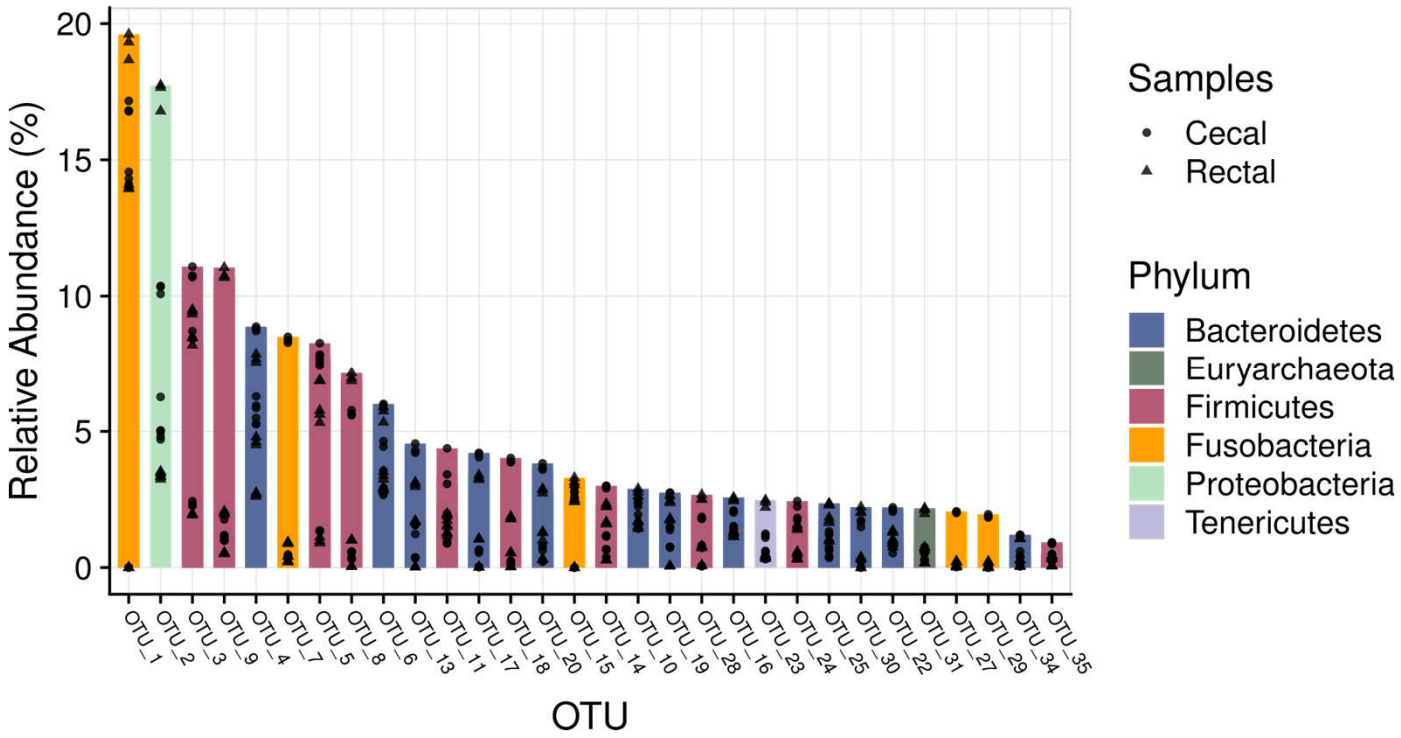

fig. S1: Top-most abundant OTUs identified by 16S target sequencing of Capybara gut in cecal and rectal samples.

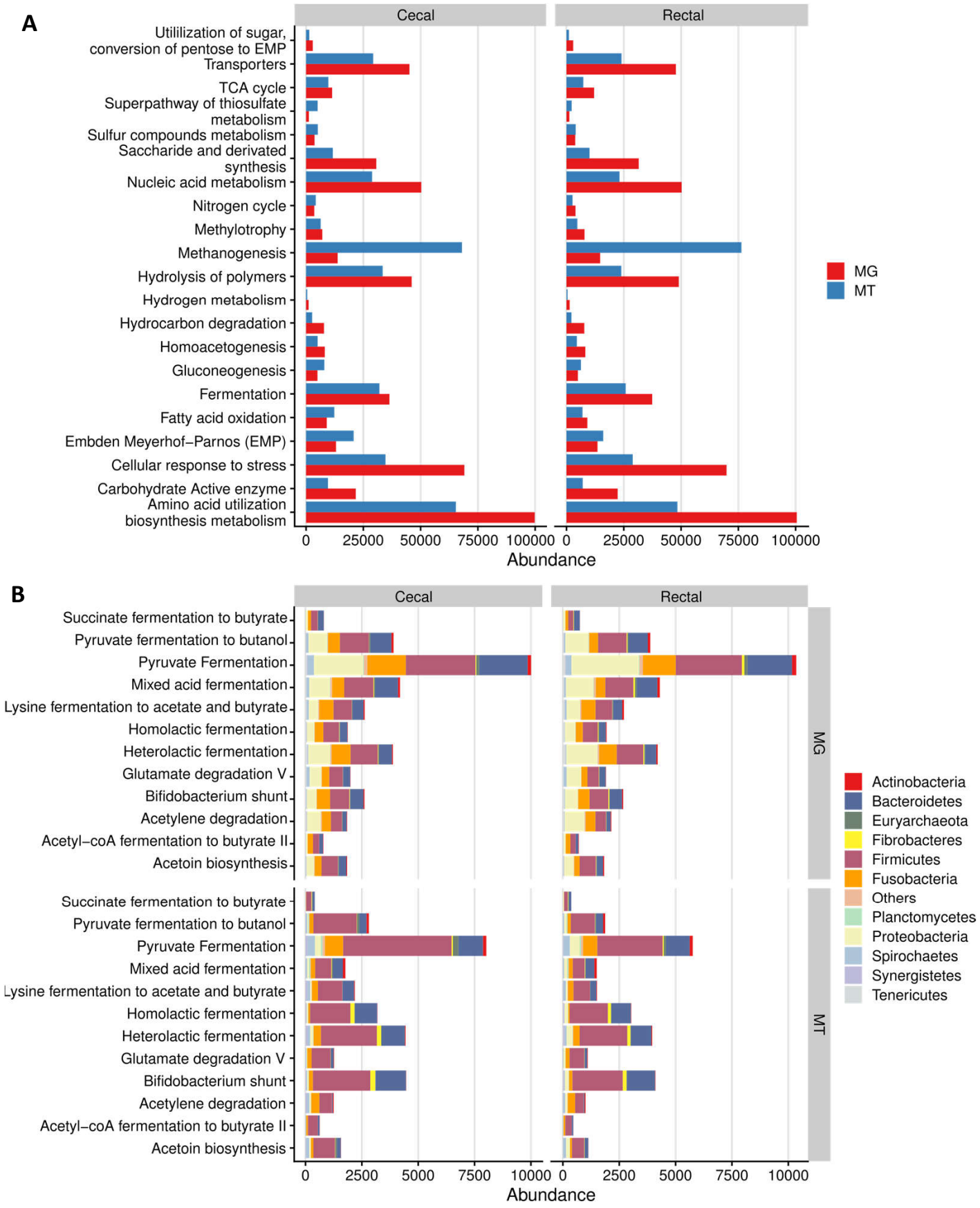

fig. S2: Functional annotation of Capybara metagenome co-assembly predicted genes according to FOAM database. **A**. Cumulative abundance of main categories. **B.** Cumulative abundance of fermentation-related categories. MG: Metagenome; MT: Metatranscriptome; Abundance is expressed as the cumulative TPM (Transcripts per Million).

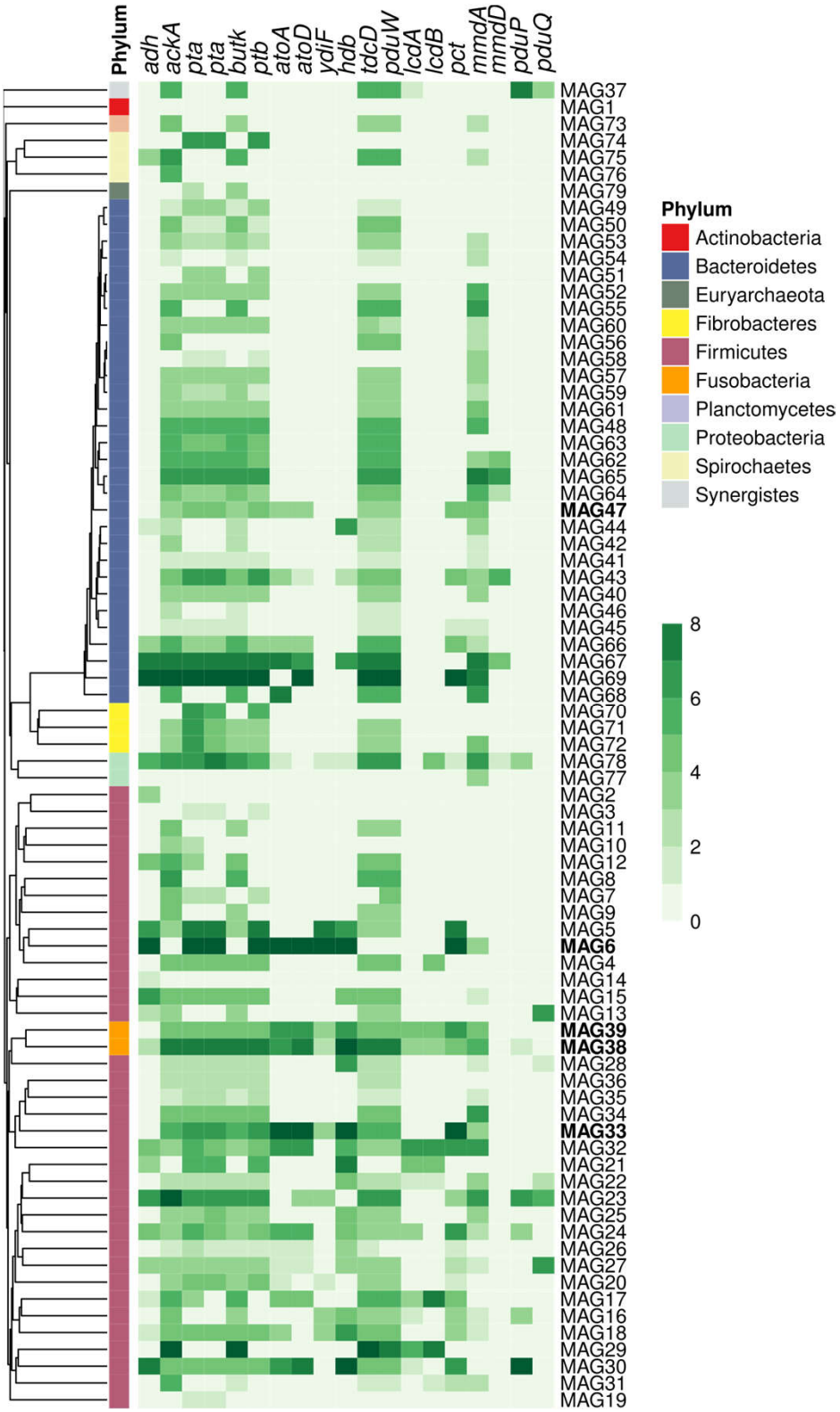

fig. S3: Summarized expression of genes related to dietary components fermentation into Short Chain Fatty Acids (SCFA). For each MAG, the expression of protein-coding genes associated with the same KO were added-up and log-normalized. Individual genes and their corresponding expression values (TPM) are shown in Supplementary Table S3. Genes encoding products *adh*: alcohol dehydrogenase; *ackA*: acetate kinase; *pta*: phosphate acetyltransferase; *butK*: butyrate kinase; *ptb*: phosphate butyryltransferase; *atoA*: Butyryl-CoA:acetate CoA-transferase; *atoD*: Butyryl-CoA:acetate CoA-transferase; *ydiF*: acetate CoA/acetoacetate CoA-transferase; *hbd*: butyryl coA dehydrogenase; *tdcD*: propionate kinase; *pduW:* propionate kinase; *lcdA*: lactoyl-CoA dehydratase subunit alpha; *lcdB*: lactoyl-CoA dehydratase subunit beta; *pct*: propionate CoA-transferase; *mmdA*: methylmalonyl coA decarboxylase; *mmdD*: methylmalonyl coA decarboxylase; *pduP:* propionaldehyde dehydrogenase; and *pduQ*: propanol dehydrogenase.

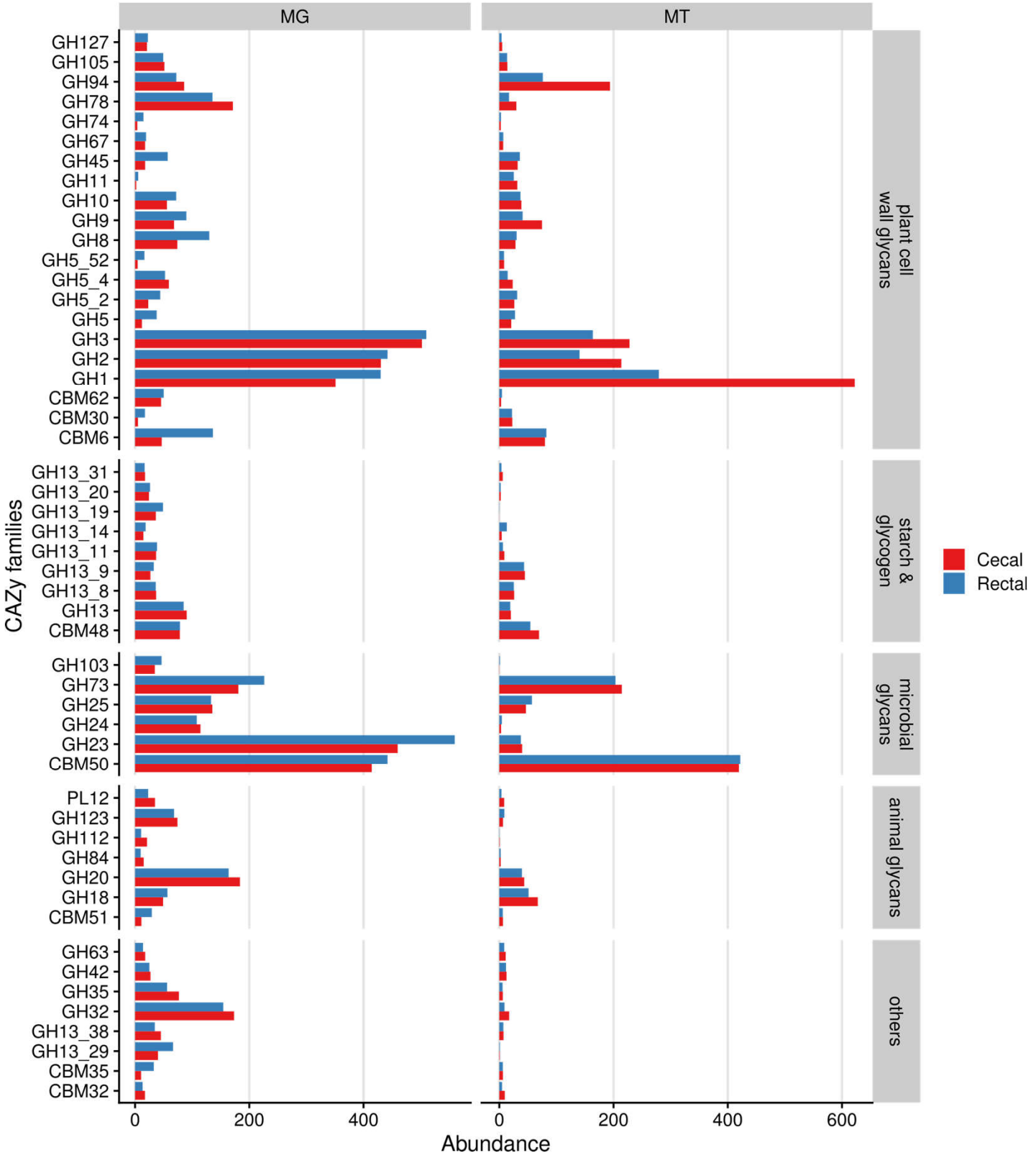

fig. S4: Functional annotation of Capybara metagenome co-assembly predicted genes according to CAZy database[62]. Cumulative Abundance of main CAZy families predicted to act on plant polysaccharides. MG: Metagenome; MT: Metatranscriptome; Abundance is expressed as the cumulative TPM (Transcripts per Million).

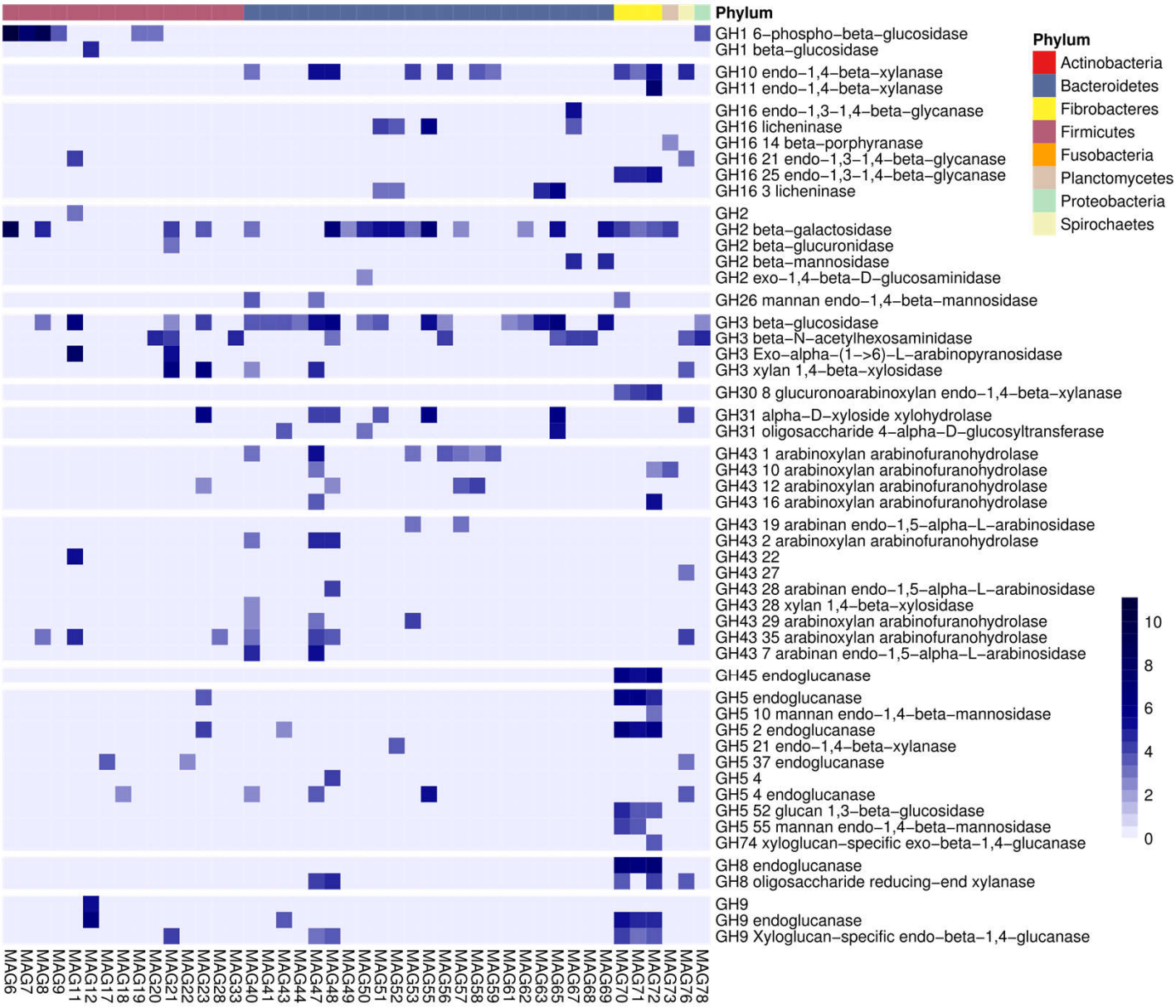

fig. S5: Summarized expression of genes predicted to act on plant polysaccharides deconstruction. For each MAG, the expression of protein-coding genes associated with the same activity within a CAZy family were added-up and log-normalized. Individual genes and their corresponding expression values (TPM) are shown in Supplementary Table S5.

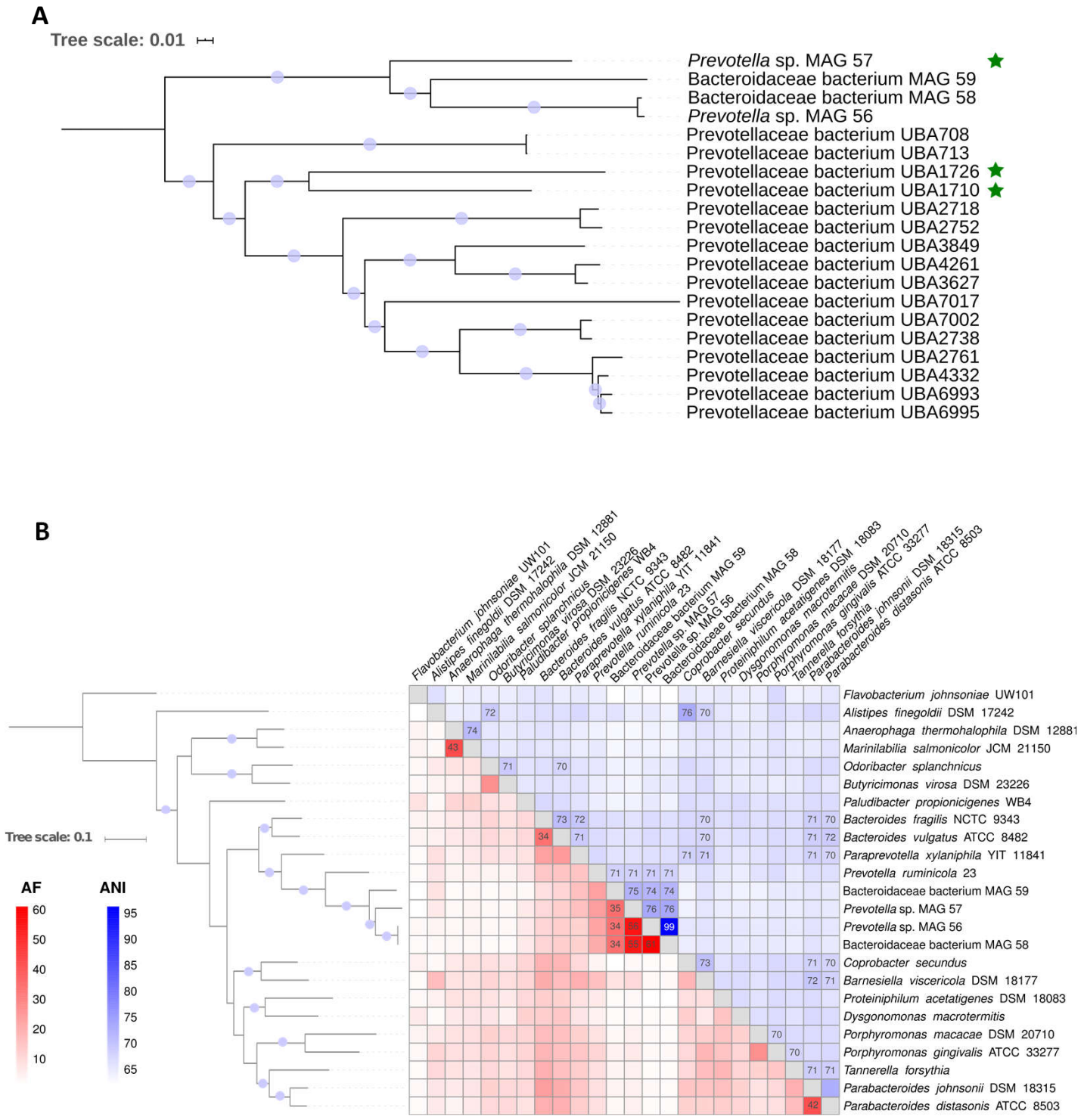

fig. S6: Genome-wide comparisons of *Prevotella* sp. MAG57 genome. **A.** Phylogenetic relationship of *Prevotella* sp. MAG57 genome and Prevotellaceae uncultured genomes recovered from UBA project[42]. Node with support values > 80 are indicated by the light blue circles. Highlighted genomes present orthologous genes to CapCBMXX-GH10. **B.** Average nucleotide identity (blue) and Alignment fraction (red) values calculated for reference Bacteroidetes and *Prevotella* sp. MAG57 genome coupled with a multi-locus phylogenetic analysis based on concatenated 92 single copy core genes according to UBCG method[69], using *Flavobetacteriaceae* as outgroup. Support values greater that 80 are shown.

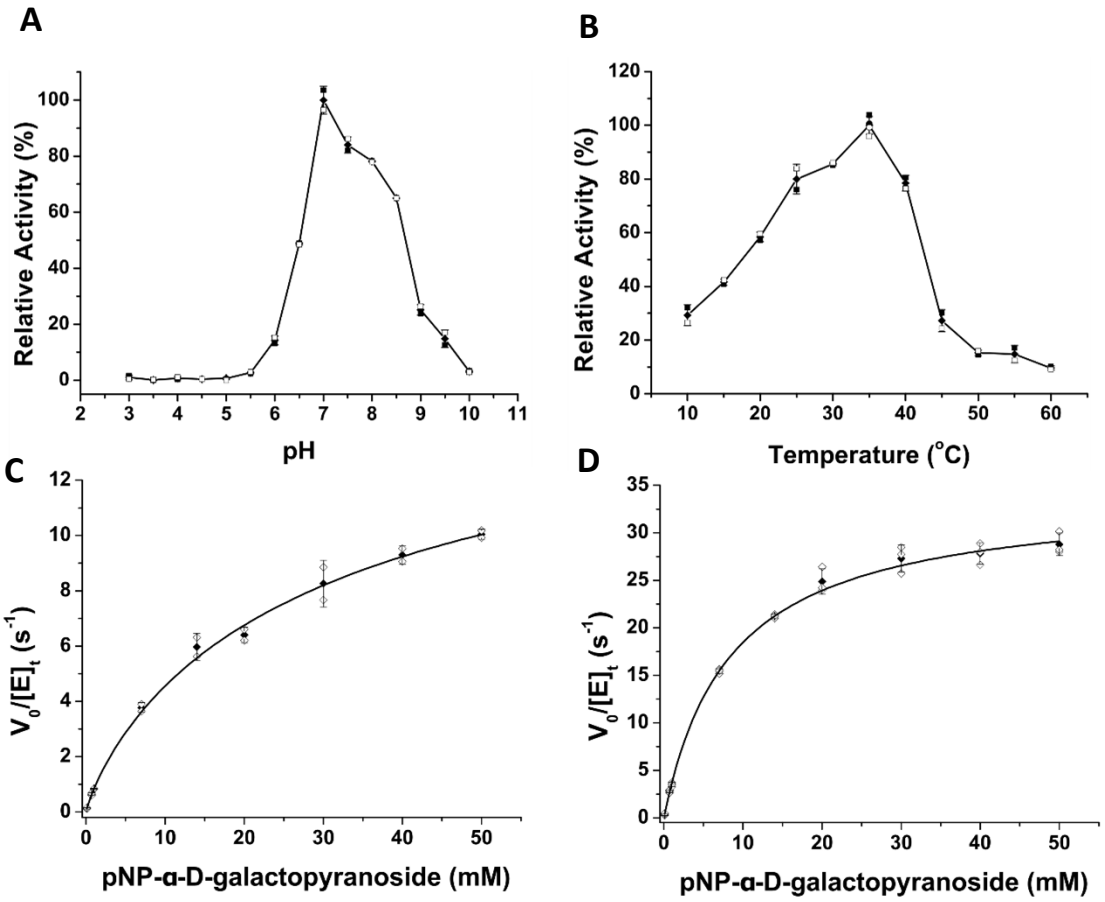

fig. S7: Biochemical and kinetic characterization of CapGH97. Effects of pH (**A**) and temperature (**B**) on relative activity. Kinetic curves of pNP-α-D-Galactopyranoside without $CaCl_2$ (**C**) and with the addition of 5 mM of $CaCl_2$ (**D**) assessed at 35°C and pH 7. The kinetic parameters are presented in Table 1. Results are expressed as mean ± SD from three independent experiments. Data points are shown as empty symbols.

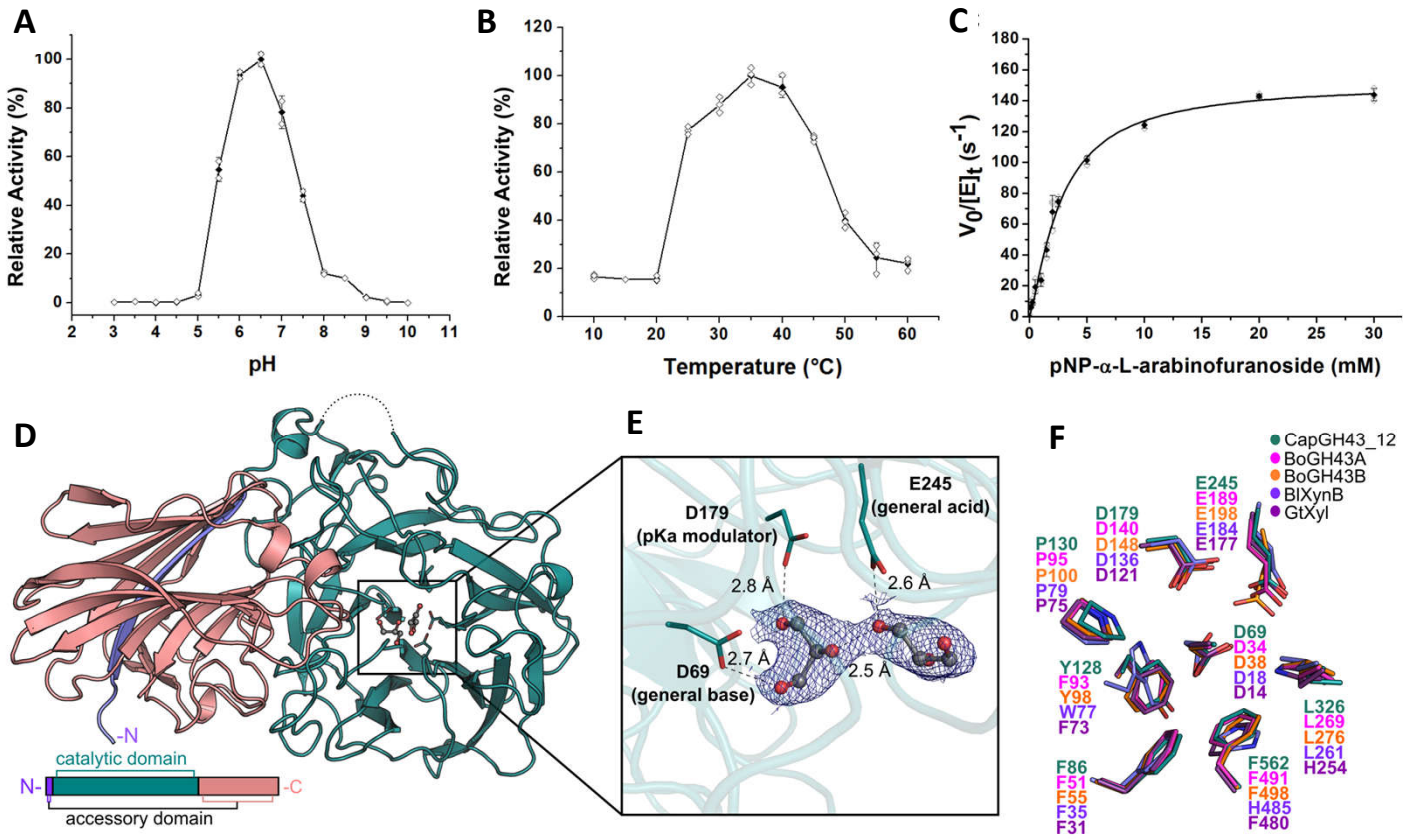

fig S8. Biochemical characterization and Structural elements of CapGH43_12. Effects of temperature (**A**) and pH (**B**) on relative activity. **C.** Kinetic curve of pNP-α-L-arabinofuranoside assessed at 35°C and pH 6.0. The kinetic parameters are presented in Table 1. Results are expressed as mean ± SD from three independent experiments. Data points are shown as empty symbols. **D.** Cartoon representation of CapGH43_12, highlighting the catalytic and accessory domains. The accessory domain is composed by β-strands from the N and C-terminus (–N and –C, respectively), as represented in the scheme (down left). **E.** CapGH43_12 active site representation, with the putative catalytic residues and pKa modulator. Two glycerol molecules are shown with $2F_o$-$F_c$electron density maps are shown with contour of 1.6 σ. **F.** Residues from the subsite −1 of GH43 subfamily 12 members from *B. ovatus* (BoGH43A and BoGH43B)[43], *B. licheniformis* (BlXynB)[44] and *G. thermoleovorans* (GtXyl) [45] .

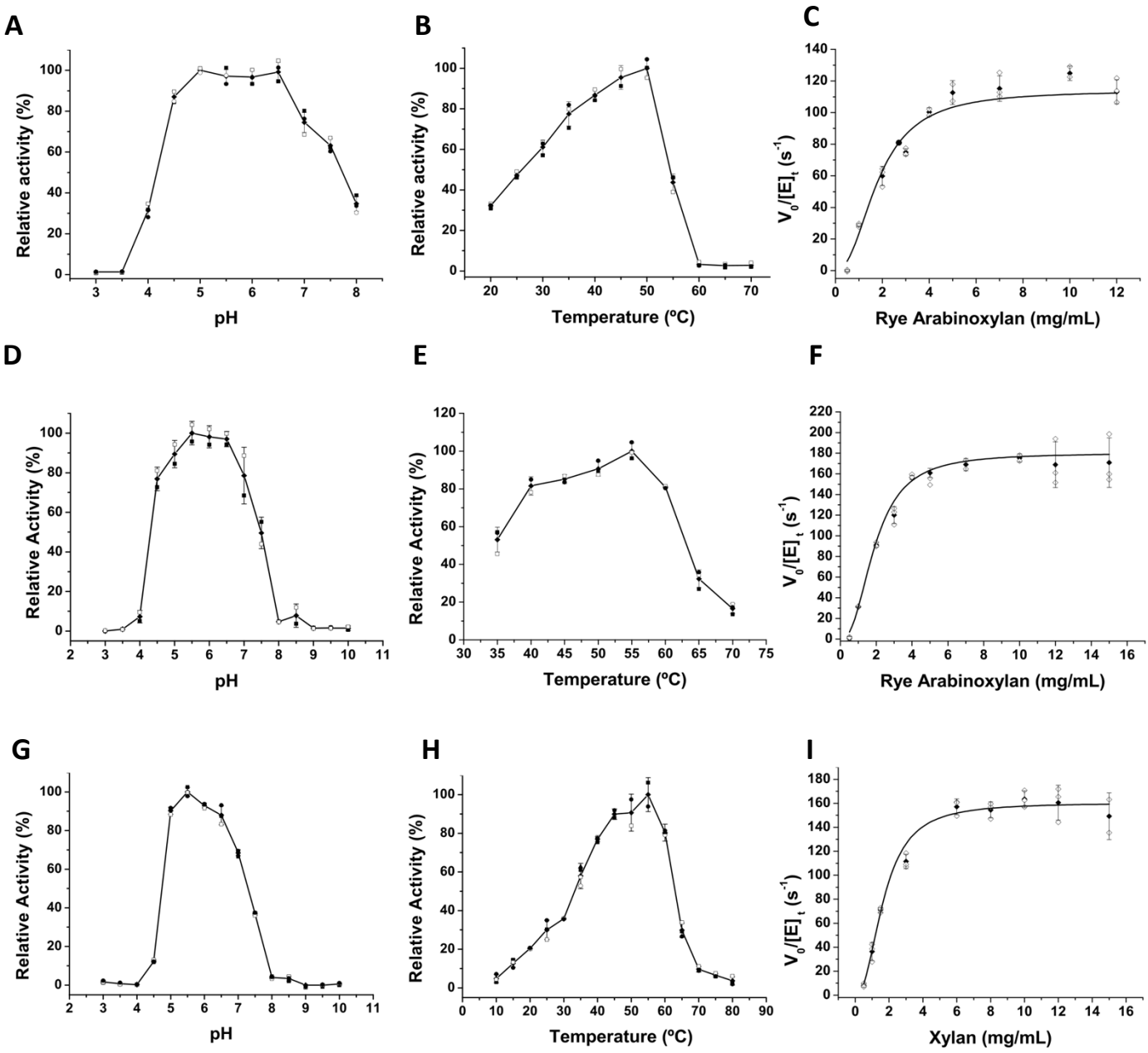

fig. S9: **Biochemical and kinetic characterization of CapCBM-GH10.** Effects of pH and temperature on relative activity and kinetic curves. **A-C.** CapGH10 full-length enzyme assayed on Rye Arabinoxylan on pH 6.0 and 45 °C. **D-F**. Xylanase CapGH10 domain assayed on Rye Arabinoxylan on pH 5.5 and 50 °C. **G-I.** Xylanase CapGH10 domain assayed on xylan beechwood on pH 5.5 and 50 °C. The kinetic parameters are presented in Table 1. Results are expressed as mean ± SD from three independent experiments. Data points are shown as empty symbols.

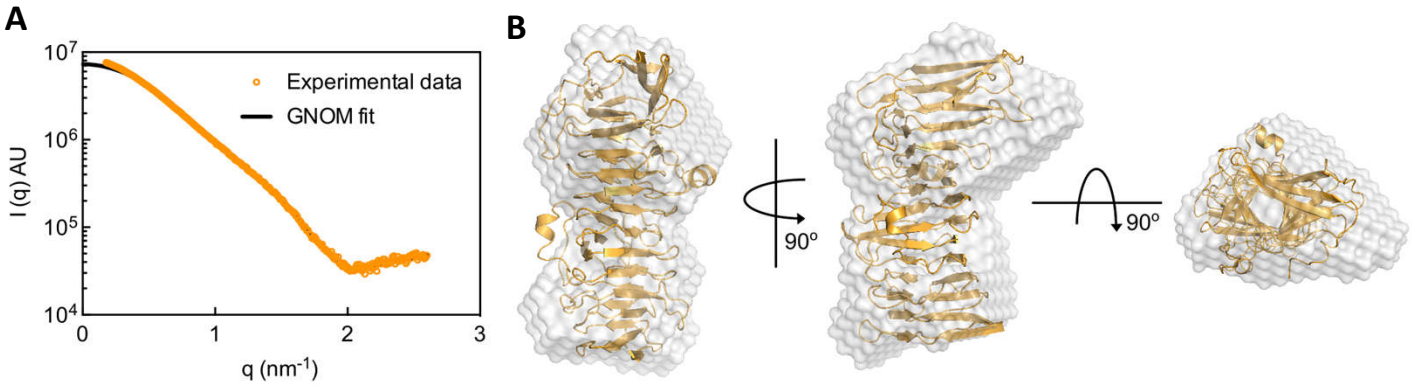

fig. S10. CapCBMXX domain is monomeric in solution. A. Experimental SAXS curve (open circles) and theoretical scattering profile (black line) computed from the P(r) function, obtained with GNOM program[86] **B.** Crystal structure of the solenoid domain fitted in the molecular envelope calculated from SAXS data.

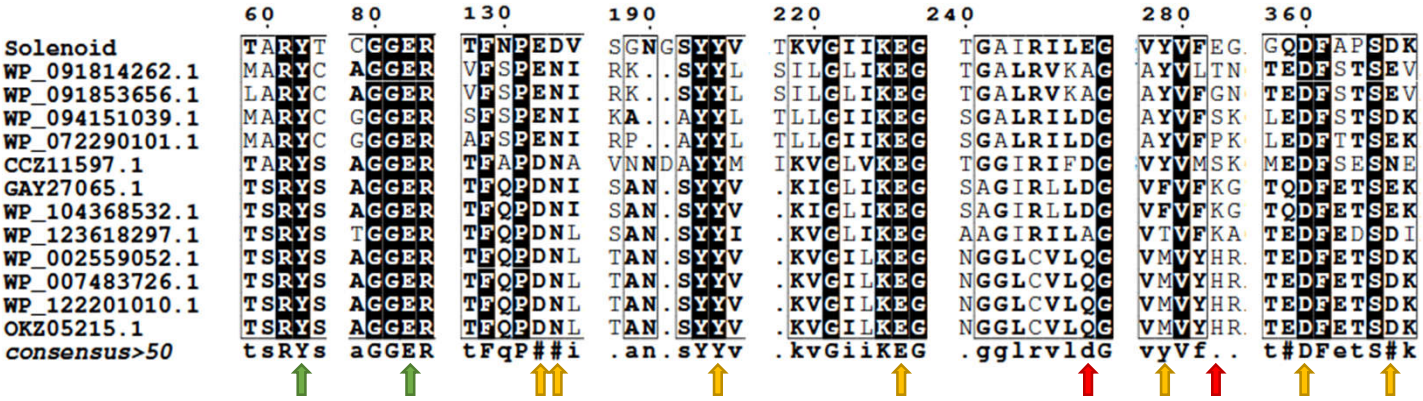

fig. S11: **Protein sequence alignment of genes with similar sequence and architecture to the investigated CapCBMXX.** The protein sequences were obtained by BLASTP search conducted with the solenoid domain solely. Only sequences containing a possibly GH10 member at C-terminus were employed for alignment and are specified as their GenBank accession code. Identical residues are highlighted by black background. Red arrows indicate residue mutations that hindered protein expression; green and yellow arrows indicate mutations that did and did not altered protein migration pattern in AGE assays, respectively. For sake of clarity, only important sequence fragments were displayed.

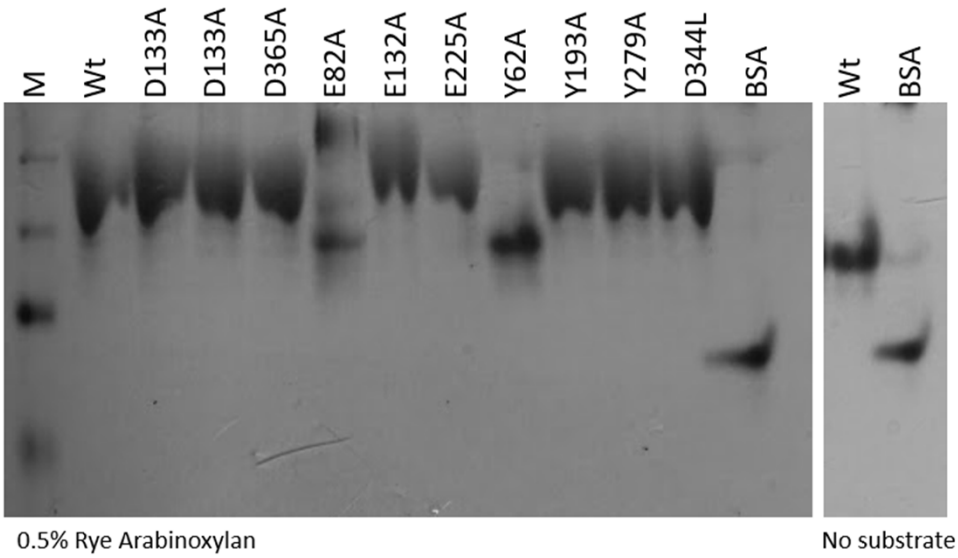

fig. S12: **Affinity gel electrophoresis (AGE) with CapCBMXX domain WT and mutants.** AGE assays were performed with the CapCBMXX domain solely and BSA as control. As the same migration pattern was observed for Rye arabinoxylan and Beechwood xylan, only results for the arabinoxylan are displayed in figure. By the same reason, only CapCBMXX WT is shown on control gel, as either WT or mutants migrate equally in AGE without substrates. M: molecular mass marker.

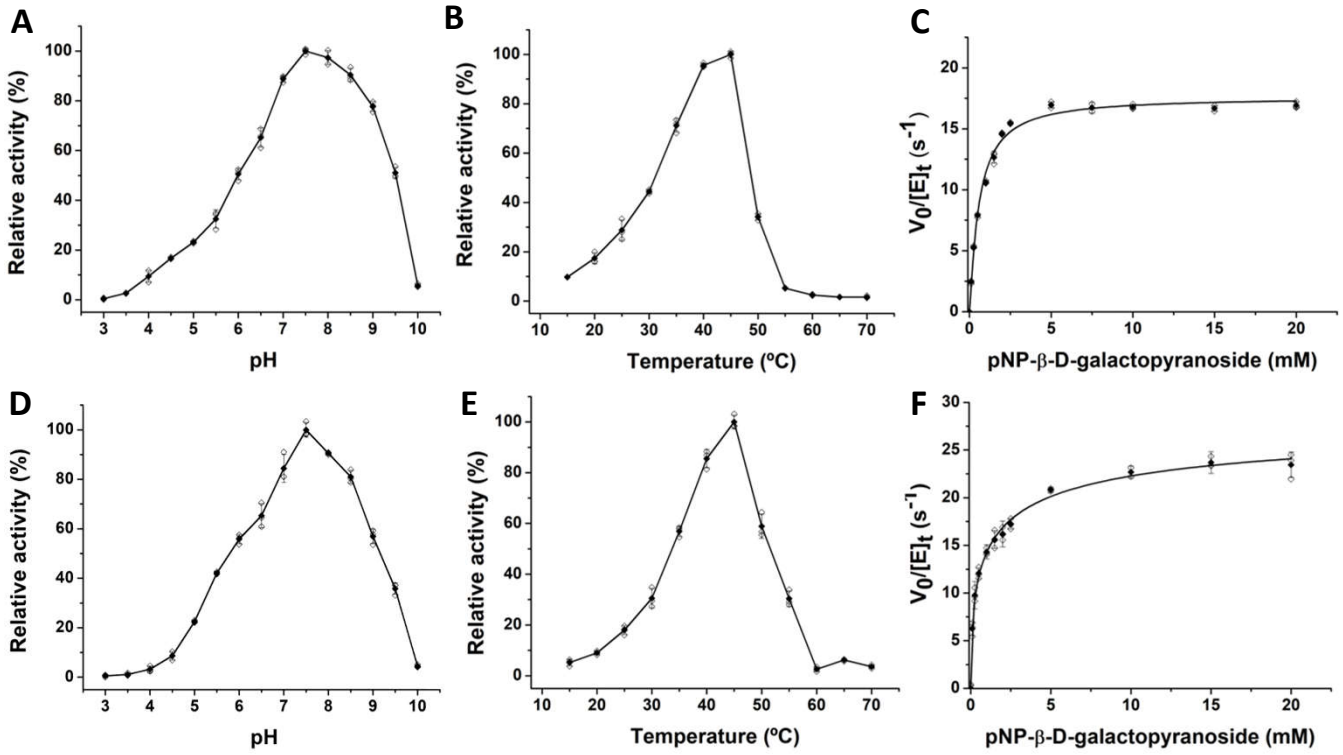

fig. S13. Biochemical and kinetic characterization of new GHXX Family. Effects of pH and temperature on relative activity and kinetic curves. **A-C.** PBMDCECB_44807 GHXXX. **D-F.** CBK67650.1. Both enzymes were assayed on pNP-β-D-Galactopyranoside on pH 7.5 and 45 °C. Kinetic parameters are presented in Table 1. Results are expressed as mean ± SD from three independent experiments. Data points are shown as empty symbols.

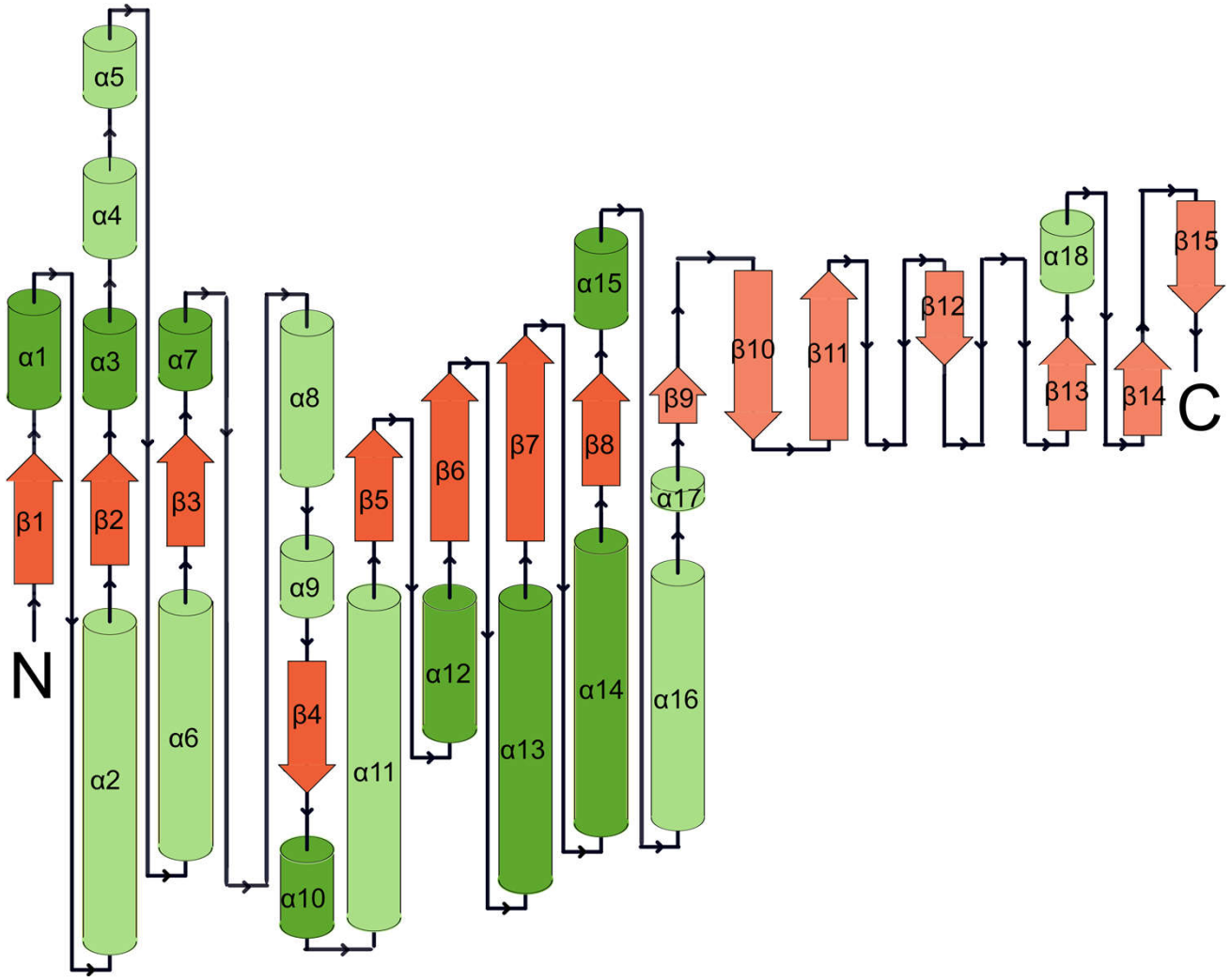

fig. S14. Structural topology of GHXXX. The TIM barrel is represented by dark colors.